Clay Minerals (2021), **56**, 46–54
doi:10.1180/clm.2021.15

CAMBRIDGE UNIVERSITY PRESS

Article

Kaolinite-armoured polyurea microcapsules fabricated on Pickering emulsion: controllable encapsulation and release performance of a lipophilic compound

Cunjun Li[1,2,3*,‡], Minghao Wang[1,‡], Zhaoliang Liu[1], Yanqi Xu[1,4,5], Chunhui Zhou[3] and Linjiang Wang[1,4,5*]

[1]College of Materials Science and Engineering, Guilin University of Technology, Guilin 541004, China; [2]Engineering Research Center of Biochar of Zhejiang Province, Hangzhou 310021, China; [3]Research Group for Advanced Materials & Sustainable Catalysis (AMSC), College of Chemical Engineering, Zhejiang University of Technology, Hangzhou 310032, China; [4]Key Lab of New Processing Technology for Nonferrous Metals and Materials Ministry of Education, Guilin 541004, China and [5]Guangxi Beibu Gulf Engineering Research Center for Green Marine Material, Guilin 54100, China

Abstract

Microcapsules are successfully used in various applications such as self-healing, drug delivery and military camouflage. The shells of the microcapsules based on the traditional surfactant-stabilized emulsion template method are often single organic materials. The surfactants generally have insufficient stability against demulsification during preparation of the microcapsules. In the present study, kaolinite was used as an emulsifier for stabilizing Pickering emulsions and subsequently as an enhancer for forming microcapsules. Kaolinite-armoured polyurea microcapsules were fabricated based on the interfacial polymerization of isophorone diisocyanate at the oil–water interfaces of kaolinite-stabilized Pickering emulsions. The prepared microcapsules with core–shell structure were spherical and exhibited good dispersibility in anhydrous ethanol. The shell thickness (~0.5–1.0 μm) and diameter (~20.0–160.0 μm) of kaolinite-armoured polyurea microcapsules may be tailored by varying the dosages of isophorone diisocyanate and kaolinite and the emulsifying speed of the high-shear homogenizer. Hence, the encapsulation and release performance of microcapsules may be controlled. The kaolinite particles were embedded and armoured in a polyurea matrix. The formed kaolinite-embedded and -armoured polyurea structures might prolong the release of the encapsulated lipophilic Sudan Red (III) from 20 to 45 h. The microcapsules have controllable encapsulation and release characteristics for lipophilic compounds and are cost effective, making them suitable pesticides.

Keywords: emulsion, interfacial polymerization, kaolinite, microcapsule, polyurea

(Received 25 December 2020; revised 6 April 2021; Accepted Manuscript online: 16 April 2021; Associate Editor: Margarita Darder)

Recently, microcapsules have been extensively investigated and used in many applications, such as in the energy storage, pharmaceutical, military camouflage and defence and agricultural industries (Zhao & Zhang, 2011; Yi *et al.*, 2015; Jiang *et al.*, 2018; Zhao *et al.*, 2020). Microencapsulation contributes to environmental protection by isolating volatile, deliquescent, oxidizable and photodegradable guest compounds from the external environment (Ravanfar *et al.*, 2018; Xiao *et al.*, 2019; Bah *et al.*, 2020).

Microcapsules can be fabricated using a variety of methods, including solvent evaporation (Asghari-Varzaneh *et al.*, 2017), spray drying (Lavanya *et al.*, 2020), sol–gel (Yin *et al.*, 2020), *in situ* polymerization (Nguon *et al.*, 2018), interfacial polymerization (Jerri *et al.*, 2016), complex coacervation (Demirbağ & Aksoy, 2016) and surfactant exchange (Chatterjee *et al.*, 2018). Among these methods, interfacial polymerization has attracted much attention because of its many advantages. This method can be easily carried out at the oil–water interface of an emulsion, and it is easy to control the extent of polymerization to produce microcapsules with various sizes and shell thicknesses. However, as conventional emulsions are usually stabilized by surfactants, the microcapsule shells formed on surfactant-stabilized emulsions are composed of organic polymer matrices with impurities of surfactant molecules. Such a composition of microcapsules has many drawbacks, such as flammability, poor thermal and chemical stability and low mechanical strength (Cai *et al.*, 2009; Li *et al.*, 2014; Kumar *et al.*, 2021). Surfactants can also be harmful to humans and the environment. Hence, using solid particles instead of surfactants to stabilize emulsions and then fabricating microcapsules on this basis is a candidate approach to overcoming the above drawbacks of microcapsules.

The use of solid particles as emulsifiers to stabilize emulsions can be traced back to the beginning of the twentieth century, which were called later Pickering emulsions (Pickering, 1907). In Pickering emulsion systems, the emulsifiers are investigated using various natural and artificial materials, such as cellulose (Dai *et al.*, 2020), carbon black (Katepalli *et al.*, 2013), silica (Hassander *et al.*, 1989) and clay minerals (Ganley *et al.*, 2017; Machado *et al.*, 2019; Gonzalez Ortiz *et al.*, 2020) and their derivatives. Solid particles used for stabilizing emulsions are low cost

*Email: cunjunlee@163.com (C Li); wlinjiang@163.com (L Wang)
‡These two authors contributed equally to this work.
Cite this article: Li C, Wang M, Liu Z, Xu Y, Zhou C, Wang L (2021). Kaolinite-armoured polyurea microcapsules fabricated on Pickering emulsion: controllable encapsulation and release performance of a lipophilic compound. *Clay Minerals* **56**, 46–54. https://doi.org/10.1180/clm.2021.15

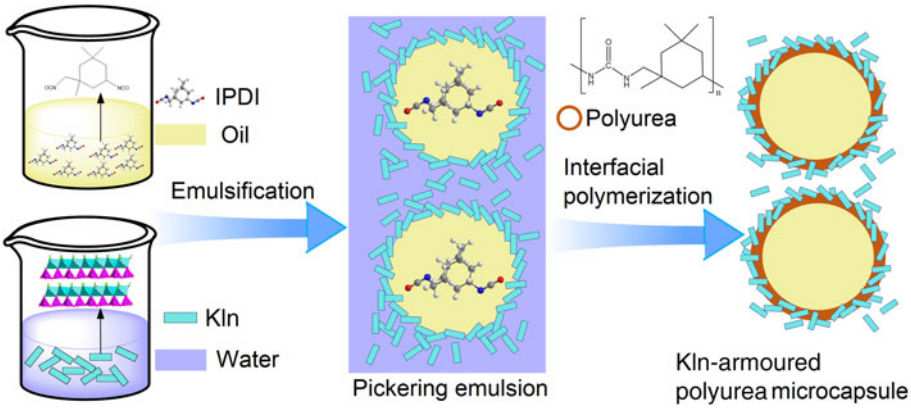

Fig. 1. Schematic of the formation of Kln-armoured polyurea microcapsules.

and environmental friendly. They improve emulsification stability and can be recovered from the emulsification system by centrifugation (Fan & Striolo, 2012; Ganley *et al.*, 2017; Yang *et al.*, 2017). This may contribute to fabricating microcapsules with fewer defects by preventing the oil–water interface destruction caused by demulsification, and it may also reduce the cost of fabricating microcapsules. Moreover, the most vital aspects in terms of determining the performance of a microcapsule are the composition and structure of its shell (Li *et al.*, 2012; Yin *et al.*, 2014). In this context, microcapsules with shells composed of polymers and solid particles can be easily fabricated based on Pickering emulsions, where the solid particles may serve as an enhancer of the performance of microcapsules.

The fabrication of microcapsules based on Pickering emulsions and the derived shells of microcapsules composed of polymers and solid particles have been reported in many studies. The solid particles used in those systems contain various organic and inorganic compounds, such as cellulose, chitosan, $CaCO_3$ and silica (Wang *et al.*, 2012; Yin *et al.*, 2014; Zhang *et al.*, 2014; Zhang *et al.*, 2018; Bago Rodriguez & Binks, 2019). Among them, silica and its modified products are the most intensively studied solid particles in the preparation of Pickering emulsions and for subsequent use in the composition of the microcapsule shell. However, most of the original particles, including silica, might not be well hybridized in the polymer matrix of the microcapsule shell, so these particles usually require additional steps for modification and improvement of their compatibility. In addition, most of these particles are spherical in shape, resulting in nondirective combination in the polymer matrix of the microcapsule shell. Therefore, in the manufacture of microcapsules, a solid particle in its original form (without modification) with affinity to the polymer matrix is desirable.

Kaolinite (Kln), as a layered clay mineral, can be used as an emulsifier in Pickering emulsion systems. Previous works of our group (Liang *et al.*, 2018; Cai *et al.*, 2019; Tang *et al.*, 2019) and other groups (Li *et al.*, 2015) have revealed that both original and modified Kln can stabilize emulsions. Because of the asymmetric structure of Kln (i.e. the octahedral surface of the platelets contains μ-hydroxy groups and the tetrahedral surface contains siloxane groups), the hybrid structure of Kln and the polymer matrix may be distinctive. To account for this, the aim of this work was to develop a novel microcapsule with a shell composition of Kln and polyurea to investigate the profile of the Kln–polyurea shell and to explore the possibility of Kln enhancing the controlled-release performance of microcapsules.

Herein, a strategy to prepare Kln–polyurea microcapsules was proposed. A schematic illustration of the preparation of such microcapsules is shown in Fig. 1. Firstly, an oil phase containing isophorone diisocyanate (IPDI) and a water phase containing Kln were prepared separately, then they were mixed in a tube, followed by emulsification with a high-shear homogenizer. After emulsification, a Kln-stabilized Pickering emulsion was obtained. Eventually, the Kln-stabilized Pickering emulsion (E_{Kln}) was used as a template for fabrication of Kln-armoured polyurea microcapsules (C_{KP}) through interfacial polymerization of IPDI at the oil–water interfaces. The Kln is hybridized with polyurea forming a Kln-embedded and armoured polyurea structure, which is beneficial for prolonging the slow release of encapsulated Sudan Red (III) (SR) from C_{KP}. This method takes full advantage of Kln as an emulsifier for Pickering emulsions and subsequently as an enhancer for microcapsule formation, and it is expected to shed light on advanced applications of clay minerals in composites.

Experimental

Materials

Kln was collected from Maoming area, China, and was purified by sedimentation to collect the <2 μm fraction (Bergaya & Lagaly, 2013). It was then used as an emulsifier to stabilize Pickering emulsions and also in the composition of the final microcapsule shell. The chemical composition (wt.%) of Kln, determined with a RIGAKU ZSX100e X-ray fluorescence (XRF) spectrometer, was as follows: SiO_2 46.71%, Al_2O_3 37.11%, Fe_2O_3 0.51%, TiO_2 0.16%, MgO 0.21%, K_2O 0.58% and Na_2O 0.11%.

IPDI (99%) and dibutyltin dilaurate (DBTDL; 95%) were purchased from Shanghai Macklin Biochemical Co., Ltd, China. Liquid paraffin (chemical grade) and anhydrous ethanol (analytical grade) were provided by Xilong Chemical Co., Ltd, China. SR was obtained from Shanghai Yuanye Biological Technology Co., Ltd, China. The water used in this work was deionized using water purification equipment (AXLB1015, Chongqing Asura Technology Development Co., Ltd, China).

Preparation of the Kln-stabilized Pickering emulsion

A total of 4 mL of the liquid paraffin was mixed with 0.4 g IPDI and 0.07 g DBTDL in a beaker with continuous stirring. The obtained mixture was then stored and used as the oil phase for the Pickering emulsion. An aqueous phase containing Kln

https://doi.org/10.1180/clm.2021.15 Published online by Cambridge University Press

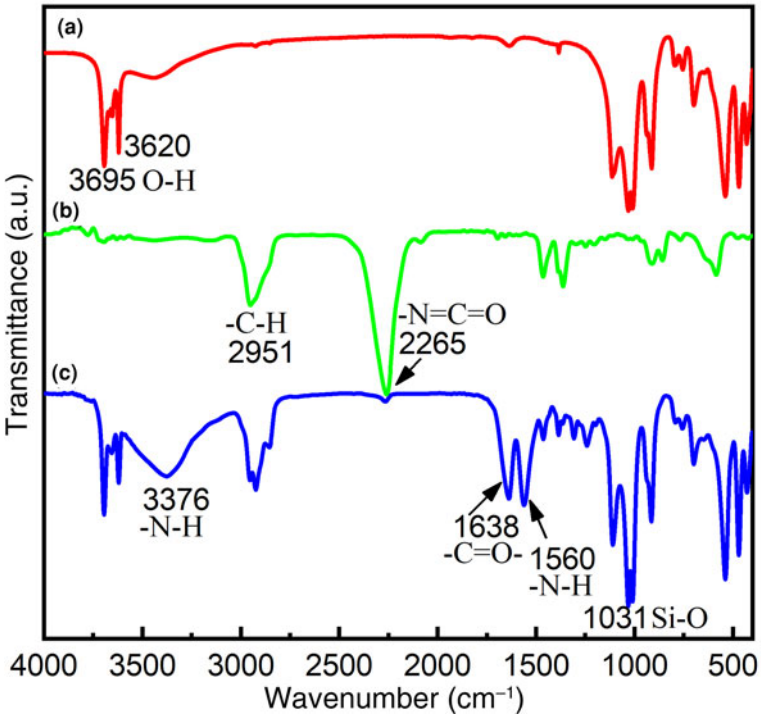

Fig. 2. FTIR spectra of (a) Kln, (b) IPDI and (c) C_{KP}.

emulsifier was produced by adding 0.4 g Kln to 16 mL deionized water and stirring for 5 min. Finally, the Kln-stabilized Pickering emulsion was prepared by blending the above oil phase and aqueous phase in a glass tube, followed by emulsification using a high-shear homogenizer (IKA-T18, IKA (Guangzhou) Instrument Equipment Co., Ltd, China) at 12,000 rpm for 3 min. The prepared sample was labelled as E_{Kln}.

Preparation of the Kln–polyurea microcapsule

To accelerate the interfacial polymerization of IPDI with water on E_{Kln} droplets, the prepared E_{Kln} was transferred to a three-necked flask and placed in a thermostat (DF-101S) at 70°C for 5 h. Subsequently, the system was adjusted to 50°C and stored for another 12 h. After the reaction was complete, the mixture was centrifuged (TDZ5-WS, Xiangyi Centrifuge Instrument Co., Ltd, China) at 4000 rpm for 5 min. The upper fraction was then separated with a separation funnel. The C_{KP} was finally obtained after washing it with deionized water to eliminate the adsorbate and drying it at 70°C for 24 h. The formed C_{KP} itself was not a pesticide, but it may be used as carrier to encapsulate lipophilic compounds including pesticides.

To tailor the shell thickness of C_{KP}, IPDI dosages of 0.3, 0.4, 0.5 and 0.6 g loaded in the oil phase were applied following the procedure used to prepare the E_{Kln}. The E_{Kln} containing various dosages of IPDI was denoted as $E_{Kln\text{-}x\text{IPDI}}$, where the subscript *x* refers to the dosage of IPDI. Similarly, the resulting corresponding C_{KP} with various shell thicknesses were denoted as $C_{KP\text{-}x\text{IPDI}}$. For example, $C_{KP\text{-}0.6\text{IPDI}}$ represents a Kln–polyurea microcapsule fabricated at an IPDI dosage of 0.6 g.

To tune the diameter of C_{KP}, the dosages of Kln and the emulsifying rates of the high-shear homogenizer for E_{Kln} were adjusted. The E_{Kln} prepared at a Kln dosage of 0.4 g and at an emulsifying speed of 12,000 rpm was denoted as $E_{0.4\text{Kln-}12r}$. Correspondingly, the C_{KP} fabricated base on $E_{0.4\text{Kln-}12r}$ was denoted as $C_{KP\text{-}0.4\text{Kln-}12r}$. Similarly, $C_{KP\text{-}0.2\text{Kln-}10r}$ and $C_{KP\text{-}0.1\text{Kln-}8r}$ were obtained.

SR was selected as the lipophilic compound encapsulated into C_{KP} to study its encapsulation and release performance. To fabricate SR-encapsulated C_{KP}, the SR was dispersed into a liquid paraffin matrix at a concentration of 1 mg mL^{-1} during the preparation of the oil phase for E_{Kln}. Then, the oil phase containing SR was used following the preparation procedure of E_{Kln} and subsequently for C_{KP}.

Characterization of the Kln-stabilized Pickering emulsion and the Kln–polyurea microcapsules

Fourier-transform infrared (FTIR) spectroscopy in the frequency range 400–4000 cm^{-1} was carried out using a Thermo Nexus 470 spectrometer and following the KBr disc method. A total of 32 scans were obtained for each sample at a resolution of 4 cm^{-1}. The morphologies and the shell thicknesses of C_{KP} were investigated using a HITACHI S-4800 scanning electron microscope (SEM). To test the shell thicknesses of C_{KP}, C_{KP} was first ground in a mortar, then washed with petroleum ether to remove encapsulated paraffin, centrifuged at 4000 rpm to obtain the solid component and finally dried and sprayed with gold. Optical micrographs of the E_{Kln} droplets and C_{KP} were obtained on a Leica DM RX-type microscope. Before observation of E_{Kln} droplets under the microscope, E_{Kln} was dropped onto a glass slide and then deionized water was added to separate the overlapped droplets. For characterization of C_{KP}, the wet C_{KP} obtained from the separating funnel after washing and before drying was placed on a glass slide and then was separated using anhydrous ethanol.

Characterization of the encapsulation and release performance of Kln–polyurea microcapsules

The encapsulation performance of SR in C_{KP} was evaluated by calculating the concentration of SR encapsulated in C_{KP} as a percentage of the initial concentration of SR in the oil phase. To

https://doi.org/10.1180/clm.2021.15 Published online by Cambridge University Press

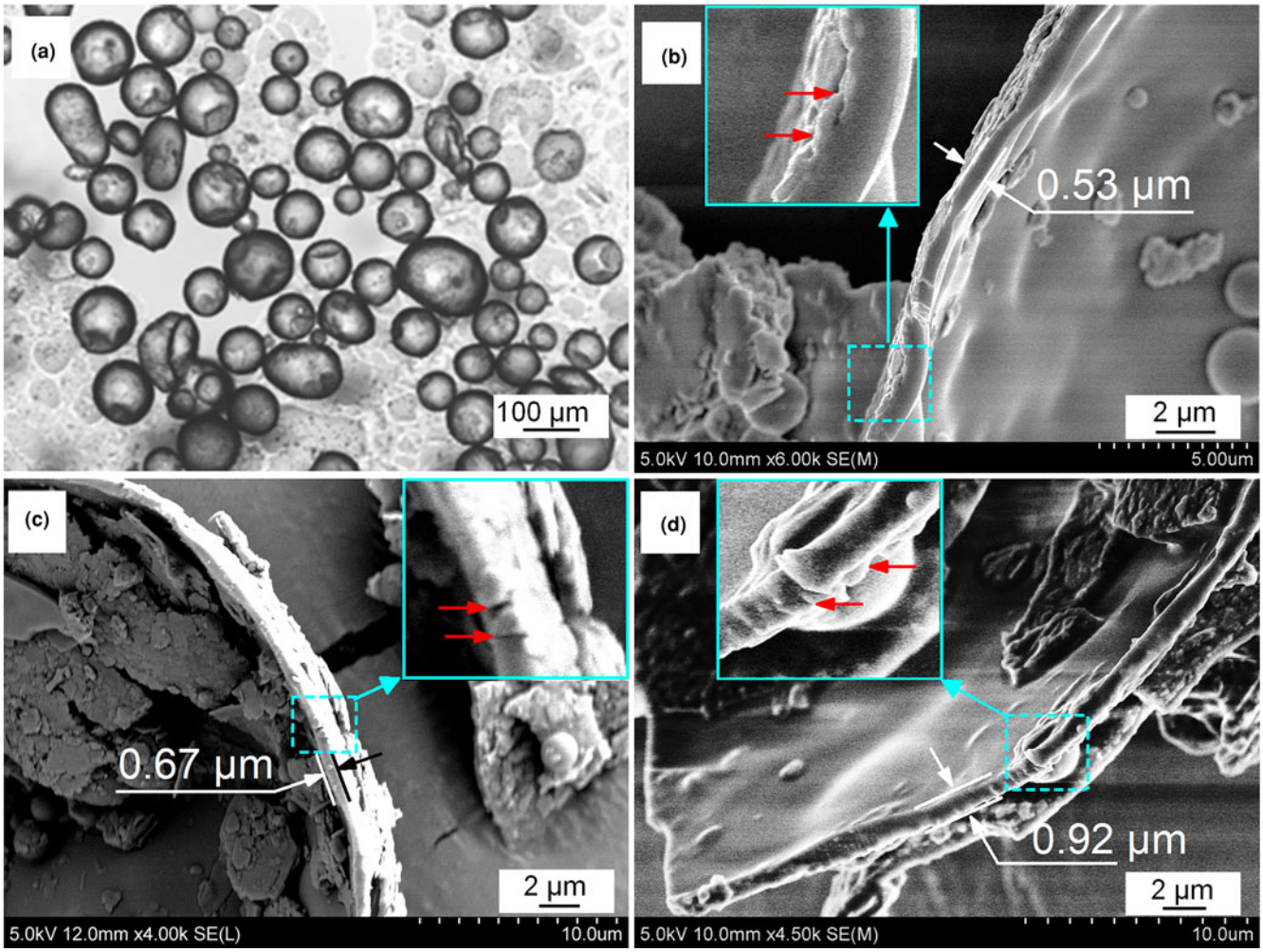

Fig. 3. Morphologies of C_{KP} fabricated at various dosages of IPDI: (a) optical micrograph of C_{KP} fabricated at an IPDI dosage of 0.3 g; SEM images of the shell profile of C_{KP} fabricated at IPDI dosages of (b) 0.3 g, (c) 0.4 g and (d) 0.5 g; the insets correspond to magnifications of the selected areas in (b), (c) and (d).

determine the concentration of SR encapsulated in C_{KP}, C_{KP} was cut open to allow for oil-phase release and then was centrifuged at 12,000 rpm to remove the shell of C_{KP}. The concentration of SR encapsulated in C_{KP} was finally obtained by testing the concentration of SR in the supernatant liquid.

The release performance of SR from C_{KP} was characterized by determining the concentration of SR in anhydrous ethanol. Specifically, 5.0 g of C_{KP} were first added into a dialysis bag (3500 Da) and then was transferred to 150 mL of anhydrous ethanol. After a certain time, 300 μL of the release medium were removed to determine the concentration of SR in anhydrous ethanol. Determination of SR was performed using a Perkins Elmer Lambda 750S UV/VIS spectrophotometer (190–2500 nm) at a wavelength of 507 nm (wavelength accuracy of ±0.15 nm).

Results and discussion

Characterization of the Kln-armoured polyurea microcapsules

C_{KP} were fabricated based on the Kln-stabilized Pickering emulsion templates. Previous work has shown that Kln was distributed in the continuous phase (water in this work) of the Pickering emulsion, forming a three-dimensional network (Liang *et al.*, 2018; Cai *et al.*, 2019; Tang *et al.*, 2019). Due to the distribution of IPDI in liquid paraffin in this work, the IPDI interaction with water was at the oil–water interface. As the reaction proceeded, formation of the polyurea bulk took place *via* polymerization of diisocyanate (–NCO) with melamine ($–NH_2$) in the emulsion system (Yi *et al.*, 2015). After the interfacial polymerization, a C_{KP} containing Kln and polyurea might have been formed.

The composition of the C_{KP} shell was investigated by characterization with FTIR. Kln and IPDI were also tested as control samples to analyse the chemical bonds in C_{KP} (Fig. 2). The characteristic bonds of polyurea in C_{KP} (Fig. 2c), which involved two bands at 3376 and 1560 cm^{-1}, assigned to the N–H stretching and deformation vibrations, respectively, were detected. Some splitting bands at ~2951 cm^{-1}, assigned to –C–H on the hexatomic ring in polyurea and the methylene groups in paraffin (Zhan *et al.*, 2016), were also identified. Furthermore, a stretching vibration typical of the –C=O– bond in polyurea was also detected at 1638 cm^{-1}. The results obtained from FTIR characterization suggested the formation of polyurea in C_{KP}.

Moreover, the chemical groups observed in Kln were also detected in C_{KP} without shift, including the Si–O stretching vibration bands at 1031 cm^{-1}, the inner-surface and internal O–H stretching vibration bands at 3695 and 3620 cm^{-1}, respectively, and bands arising from metal–oxygen (metal–hydroxyl) vibrations in the lattice of Kln at <800 cm^{-1} (Fig. 2a) (Li *et al.*,

https://doi.org/10.1180/clm.2021.15 Published online by Cambridge University Press

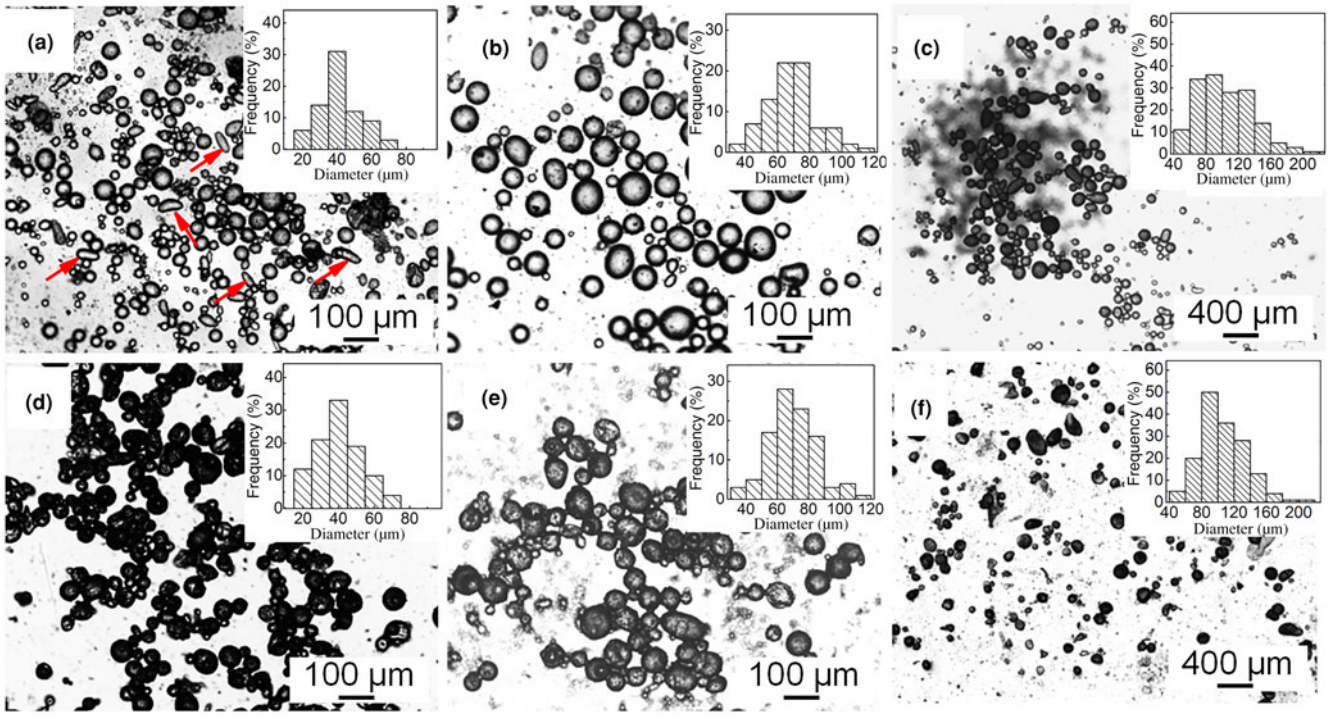

Fig. 4. Optical micrographs of (a–c) E_{Kln} and (d–f) C_{KP} fabricated at various dosages of Kln and emulsifying speeds: (a, d) 0.4 g and 12,000 rpm; (b, e) 0.2 g and 10,000 rpm; (c, f) 0.1 g and 8000 rpm; the insets correspond to the diameter distributions of C_{KP} in (d), (e) and (f).

Table 1. Encapsulation efficiencies (*EE*) of SR in various C_{KP} formulations, and the diameters and shell thicknesses of SR-encapsulated C_{KP} formulations.

Sample[a]	$C_{KP\text{-}0.3IPDI}$	$C_{KP\text{-}0.4IPDI}$	$C_{KP\text{-}0.5IPDI}$	$C_{KP\text{-}0.6IPDI}$/$C_{KP\text{-}0.4Kln\text{-}12r}$[b]	$C_{KP\text{-}0.2Kln\text{-}10r}$	$C_{KP\text{-}0.1Kln\text{-}8r}$
EE (%)	85.4	78.5	73.6	76.2	79.8	88.4
Diameter[c]	62.1	56.8	55.4	42.0	69.8	106.1
ST[d]	0.5	0.7	0.9	1.0	0.9	0.9

[a] The samples are SR-encapsulated C_{KP} formulations.
[b] $C_{KP\text{-}0.6IPDI}$ and $C_{KP\text{-}0.4Kln\text{-}12r}$ are the two marks of the same sample.
[c] As the diameter of SR-encapsulated C_{KP} formulations is polydisperse, the given diameter is the average statistic of the area observed under the optical microscope. The diameter of C_{KP} encapsulated with SR is smaller than that of C_{KP} without SR (unit: μm).
[d] ST = shell thickness. As SR-encapsulated C_{KP} has a wide ST distribution, the given values are an approximations (unit: μm).

2015). In addition, a weak band at 2265 cm^{-1} associated with the –N=C=O group was identified in C_{KP}; the same band with higher intensity was also detected in IPDI (Fig. 2b). These results suggest that the C_{KP} was composed of Kln and polyurea with no chemical bonds between Kln and polyurea, and that some unreacted IPDI remained in C_{KP}.

To further ascertain the role of the Pickering emulsion for C_{KP} formation and to investigate the mechanism of Kln hybridization with polyurea, a group of C_{KP} were fabricated at a fixed Kln amount of 0.4 g and an emulsifying speed of 1200 rpm and with IPDI dosages at 0.3, 0.4 and 0.5 g. The obtained C_{KP} were characterized using optical microscopy and SEM. The $C_{KP\text{-}0.3IPDI}$ was well dispersed in anhydrous ethanol and was spherical in shape (Fig. 3a). A total of 90% of the diameter of $C_{KP\text{-}0.3IPDI}$ was distributed within the range of 46.5–113.2 μm (counts in the viewing area), with an average diameter being ~86.4 μm. The shell thickness of $C_{KP\text{-}0.3IPDI}$ was 0.53 μm (Fig. 3b). Compared with $C_{KP\text{-}0.4IPDI}$ and $C_{KP\text{-}0.5IPDI}$, the shell thicknesses increased to ~0.67 and 0.92 μm, respectively (marked in Fig. 3c,d), suggesting that the shell thickness of C_{KP} might be tailored by varying the dosage of IPDI. Based on this approach, the encapsulation and release performance of C_{KP} might be controlled by tailoring the shell thickness.

Furthermore, the SEM images of $C_{KP\text{-}0.3IPDI}$, $C_{KP\text{-}0.4IPDI}$ and $C_{KP\text{-}0.5IPDI}$ show a smooth internal surface and a rough external surface (Fig. 3b–d). Such a phenomenon is ascribed to the habitation where Kln particles distributed in the previous E_{Kln}. That is, most of the Kln particles are distributed in the aqueous phase of E_{Kln}, while fewer Kln particles are dispersed in the oil phase. As a result, more Kln particles hybridized with the polyurea shell towards the side of the water phase. The insets in Fig. 3b–d are the corresponding magnifications of the selected areas. As indicated by the arrows in these insets, some Kln platelets are embedded and assembled within the polyurea matrix, forming a Kln-armoured polyurea shell. This combination of Kln with polyurea suggests that the Pickering emulsion acted as a template during the formation of the Kln-armoured polyurea shell. In addition, such a Kln-armoured polyurea shell may be beneficial for tuning its encapsulation and release performance.

The microcapsule size is another major factor that affects its encapsulation and release performance (Rule *et al.*, 2007; Zhao *et al.*, 2019). Previous studies have shown that the amount of

https://doi.org/10.1180/clm.2021.15 Published online by Cambridge University Press

emulsifier and shear force are the main parameters affecting the size of the emulsion droplets, thereby determining the size of the microcapsules (Yow & Routh, 2009; Ozturk *et al.*, 2015). Herein, both the dosage of Kln and the emulsifying speed of the high-shear homogenizer were varied to tailor the size of the E_{Kln} during emulsion preparation. On this basis, the sizes and morphologies of the E_{Kln} and those derived from C_{KP} were further investigated.

The optical micrographs of selected E_{Kln} in various sizes prepared under certain dosages of Kln and emulsifying speeds are shown in Fig. 4a–c. Most of the Kln particles were distributed around the oil droplets to reduce the tension at the oil–water interface and to protect the emulsion against coagulation. Meanwhile, a small number of Kln particles were dispersed in the aqueous phase because of the hydrophilicity of Kln particles (Dickinson, 1994; Liang *et al.*, 2018). Compared to the shapes of oil droplets in these emulsions, some of the oil droplets in $E_{0.4Kln\text{-}12r}$ at a high dosage of Kln (0.4 g of Kln in 16 mL water and 4 mL paraffin) and a high emulsifying speed (12,000 rpm) are non-spherical, as indicated by the arrows in Fig. 4a. In contrast, the oil droplets in $E_{0.2Kln\text{-}10r}$ and $E_{0.1Kln\text{-}8r}$ were almost entirely spherical in shape. This suggests that a high dosage of Kln and a high emulsifying speed produced non-spherical droplets in the Kln-stabilized emulsion system. As a result, some non-spherical C_{KP} particles were formed (e.g. $C_{KP\text{-}0.4Kln\text{-}12r}$ in Fig. 4d). Due to aggregation of Kln particles, the individual microcapsules were more easily aggregated for $C_{KP\text{-}0.4Kln\text{-}12r}$ when compared with $C_{KP\text{-}0.2Kln\text{-}10r}$ and $C_{KP\text{-}0.1Kln\text{-}8r}$ (Fig. 4d–f).

As C_{KP} was derived from E_{Kln}, the size of C_{KP} was determined by the size of the oil droplets in E_{Kln}. The diameters of the C_{KP} and the oil droplets in E_{Kln} were statistically analysed. Both the C_{KP} and the oil droplets in E_{Kln} are polydisperse (Fig. 4). The diameters of $E_{0.4Kln\text{-}12r}$ and $C_{KP\text{-}0.4Kln\text{-}12r}$ were in the range of 20–60 μm, those of $E_{0.2Kln\text{-}10r}$ and $C_{KP\text{-}0.2Kln\text{-}10r}$ were in the range of 50–90 μm, while those of $E_{0.1Kln\text{-}8r}$ and $C_{KP\text{-}0.1Kln\text{-}8r}$ were in the range 80–140 μm (insets of Fig. 4a–f). Interestingly, the average diameters of the oil droplets in $E_{0.4Kln\text{-}12r}$, $E_{0.2Kln\text{-}10r}$ and $E_{0.1Kln\text{-}8r}$ were ~41.3, 68.9 and 105.1 μm, respectively, while the average diameters of the correspondingly derived C_{KP} were ~42.0, 69.8 and 106.1 μm, respectively (i.e. they were larger by ~0.7, 0.9 and 1.0 μm than those of E_{Kln}). Such an increase in diameter of C_{KP} is in agreement with the shell thickness measured from SEM images (Fig. 3b–d), further confirming the formation of Kln-armoured polyurea shells upon Pickering emulsion templates *via* interfacial polymerization.

Based on the above discussion, control of the dosages of IPDI and Kln and the emulsifying speed of the high-shear homogenizer are effective approaches to tailoring the shell thickness and the size of C_{KP}. This method may be promising for the tuning of encapsulation and release performance for the fabricated C_{KP}.

Tuning of encapsulation and release performance through tailoring of the diameter and shell thickness of Kln-armoured polyurea microcapsules

With Kln serving as an emulsifier, oil-in-water Pickering emulsions were obtained at the oil volume fraction (V_{oil} / (V_{oil} + V_{water})) of 0.2 in present study. Pickering emulsions with the dispersed oil phases were the precursors for microcapsule preparation; the encapsulated substances in those derived microcapsules were oil phases. Thus, the C_{KP} might be used to carry lipophilic guests. In view of the abovementioned strategies for tailoring the diameter and shell thickness of C_{KP}, the encapsulation and release performance might be effectively tuned.

SR, a chemical dye, was selected as the lipophilic guest and was eventually encapsulated in C_{KP}. In the system in which C_{KP} is used to encapsulate SR, the encapsulation performance of SR in C_{KP} was evaluated by calculating the concentration of SR encapsulated in C_{KP} as a percentage of the initial concentration of SR in the oil phase (Eq. 1).

$$EE = \frac{c_1}{c_0} \tag{1}$$

where c_1 is the concentration of SR encapsulated in C_{KP} and c_0 is the initial concentration of SR in the oil phase.

The encapsulation efficiencies (*EE*) of SR in C_{KP} with various shell thicknesses and diameters were calculated using Eq. 1 (Table 1). The *EE* of SR in $C_{KP\text{-}x\text{IPDI}}$ decreased from 85.4% to 76.2% with increasing shell thickness from ~0.5 to ~1.0 μm. This might be ascribed to the fact that a high concentration of IPDI reacted more vigorously and rapidly with water than low concentrations of IPDI, so that the spreading rate of SR in the oil phase with a high concentration of IPDI was faster than that with low concentration of IPDI. In addition, as the shell thickness of $C_{KP\text{-}x\text{IPDI}}$ increased with increasing concentration of IPDI, the thicker shell of $C_{KP\text{-}0.6\text{IPDI}}$ could hold more SR. Consequently, the concentration of SR encapsulated in the oil phase of C_{KP} decreased with the increase in the shell thickness of C_{KP}.

Tailoring the diameter of C_{KP} is another approach for tuning the *EE* of SR in C_{KP}. As the diameter of C_{KP} increased from ~42.0 μm ($C_{KP\text{-}0.4Kln\text{-}12r}$) to 106.1 μm ($C_{KP\text{-}0.1Kln\text{-}8r}$), the *EE* of SR in C_{KP} increased from 76.2% to 88.4%. This increase may be due to the fact that the larger the diameter of C_{KP}, the greater the volume of the oil phase inside the microcapsule, and thus the higher the amount of SR. Alternatively, more SR was adsorbed by high dosages of Kln (0.4 g Kln for $C_{KP\text{-}0.4Kln\text{-}12r}$) during the emulsifying process, so that the residual amount of SR in $C_{KP\text{-}0.4Kln\text{-}12r}$ was less than that encapsulated in $C_{KP\text{-}0.2Kln\text{-}10r}$ and $C_{KP\text{-}0.1Kln\text{-}8r}$.

To study the release kinetics of SR from C_{KP}, the Korsmeyer–Peppas model (Korsmeyer *et al.*, 1983; Ritger & Peppas, 1987) was applied to analyse the experimental data (Eq. 2):

$$kt^n = \frac{M_t}{M_\infty} \tag{2}$$

where M_t/M_∞ is the released SR fraction at time t, k is the diffusion kinetic constant and n is the diffusion exponent of the SR transport mechanism. Diffusion exponent n values equal to 0.5 indicate Fickian diffusion as the SR release mechanism; n values between 0.5 and <1.0 are indicative of an anomalous SR release mechanism; for n values equal to 1.0, the SR release mechanism belongs to case II transport with zero-order release; for n values greater than 1.0, the SR release mechanism is related to super case II transport; and finally, n values <0.45 are most commonly observed in cylindrical matrices (Tsoi, 2013).

Dialysis is a commonly used method to evaluate the release performance of sustained-release materials (Amatya *et al.*, 2013; Weng *et al.*, 2020). In this work, anhydrous ethanol was used as a medium for SR release from C_{KP}. The SR-encapsulated C_{KP} with various shell thicknesses and diameters were set as the drug carriers to allow the release of SR in anhydrous ethanol. The SR release data from different C_{KP} were fitted using Eq. 2,

https://doi.org/10.1180/clm.2021.15 Published online by Cambridge University Press

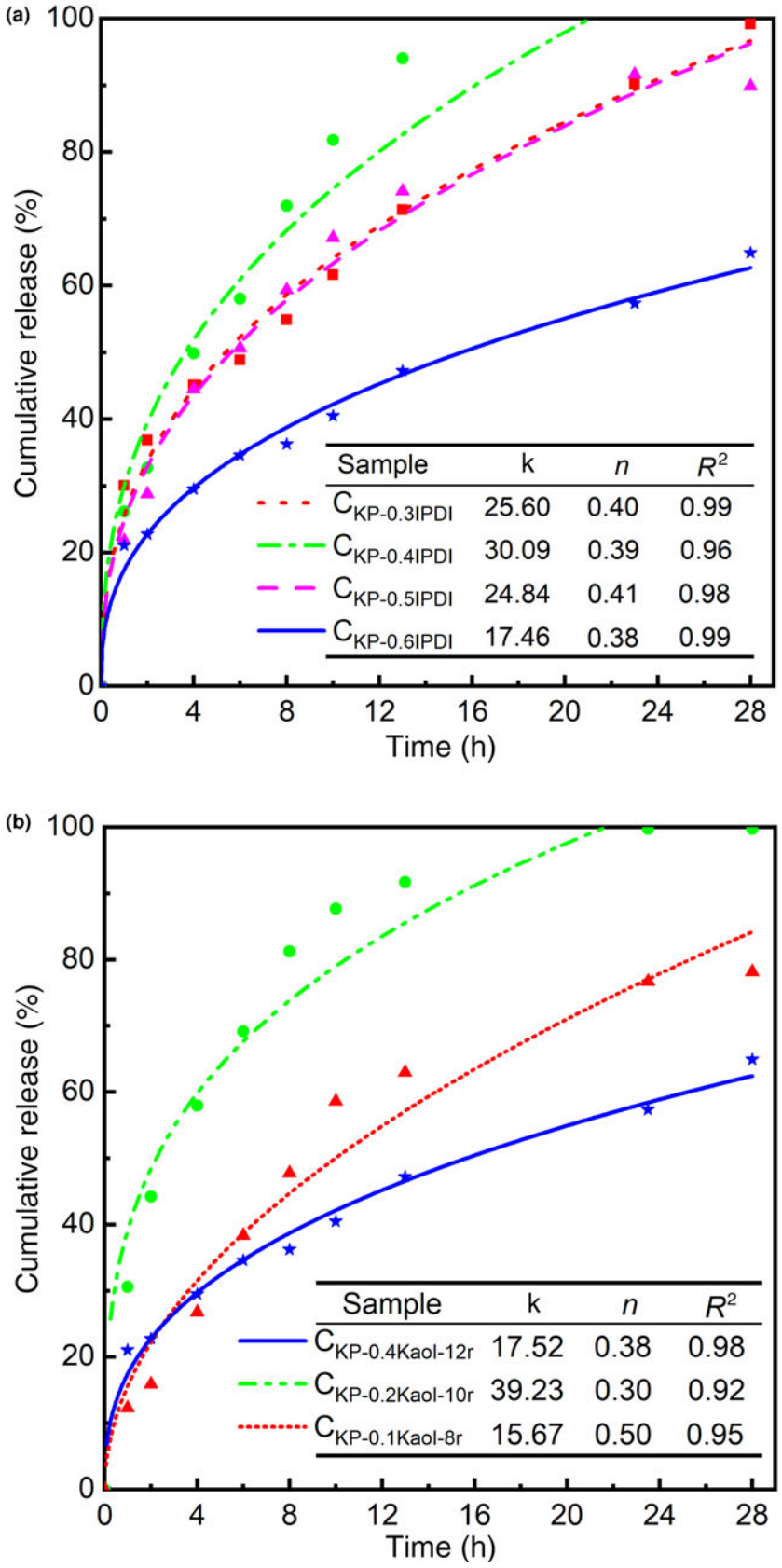

Fig. 5. Release kinetics of SR from C_{KP} with various (a) shell thicknesses and (b) diameters.

and the release kinetic parameters are given in Fig. 5a,b. The kinetic data for C_{KP} with various shell thicknesses can be nicely fitted by Eq. 2, as evidenced by the high values of R^2 (>0.96). In contrast, the fitting of the kinetic data for C_{KP} of various diameters is less satisfactory than that for C_{KP} of various shell thicknesses (R^2 >0.92).

https://doi.org/10.1180/clm.2021.15 Published online by Cambridge University Press

$C_{KP\text{-}0.6IPDI}$ shows a lower k value than those C_{KP} with thinner shell thicknesses. In particular, k was reduced drastically from $C_{KP\text{-}0.5IPDI}$ (24.84) to $C_{KP\text{-}0.6IPDI}$ (17.46). Except for the increase in the shell thickness itself, the shell structure of Kln-embedded and -armoured polyurea might be the other critical reason for the observed decrease. As the diameter of the Kln ranged from 0.2 to 2.0 μm, when the shell thickness of C_{KP} increased from a few tenths of a micron to >1 μm, Kln platelets would embed in or armour the polyurea matrix more efficiently. The Kln-armoured polyurea structure caused diffusion of SR from the internal surface to the external surface, following a zigzag path rather than a linear path to bypass the Kln platelets in the polyurea matrix.

In the release system of C_{KP}, the *n* values are >0.5, indicating that the SR release mechanism does not conform to anomalous and super case II transport. As the values of *n* are <0.45 for all C_{KP} with various shell thicknesses, the release models in those C_{KP} are similar to those in cylindrical matrices. Unexpectedly, the *n* vale in the $C_{KP\text{-}0.1Kln\text{-}8r}$ release system is equal to 0.5, conforming to Fickian diffusion. Even so, the release model is quite complicated and needs to be explored further. This is because the C_{KP} was not a pure polymer–drug system but rather a core–shell system, and its shells are organic–inorganic hybrid compounds (Kln hybridized with polyurea). Hence, several parameters, including the electrostatic interactions, ionic strength and concentration (Prasannan *et al.*, 2014), should be considered.

In practice, to reduce the dose frequency, prolonged release of a drug is usually desirable. Herein, the released rate of SR from all C_{KP} is rapid, occurring within 4 h, and the complete release of SR from C_{KP} can be controlled at from 20 to 45 h (22% SR remained not given for $C_{KP\text{-}0.6IPDI}$). The sudden release of SR in the first 4 h might be ascribed to the following two reasons: first is the large concentration difference between SR inside and SR outside of the C_{KP} in the period of its initial release; and second is the SR adsorbed on the shell of the C_{KP} released in the first period of time when the C_{KP} was placed in anhydrous ethanol. The prolonged release of SR from C_{KP} might be attributed to the Kln-armoured polyurea shell structure of C_{KP}, as evidenced by the shell profiles of C_{KP} in SEM images (Fig. 3b–d).

The aforementioned discussion suggests that the encapsulation and release performance of C_{KP} might be effectively tuned through tailoring the diameters and shell thicknesses of C_{KP}, achieved by varying the dosages of IPDI and Kln and the emulsifying speed during the preparation of Kln-stabilized Pickering emulsions.

Conclusions

Core–shell C_{KP} were fabricated by interfacial polymerization in a Kln-stabilized Pickering emulsion. Kln was hybridized with polyurea, forming a Kln-embedded- and -armoured polyurea structure. The fabricated C_{KP} has good dispersibility in anhydrous ethanol and is spherical. Control of the dosages of IPDI and Kln and the emulsifying speed of the high-shear homogenizer in the emulsifying system are effective for tailoring the shell thickness and diameter of C_{KP}. The shell thickness of C_{KP} can be tailored from ~0.5 to 1.0 μm and the diameter of the microcapsules can be tuned from ~20.0 to 160.0 μm.

By tailoring the shell thickness and the diameter of C_{KP}, the encapsulation and release performance of liposoluble compounds in C_{KP} may also be tuned. When lipophilic SR was encapsulated in C_{KP}, the C_{KP} exhibited excellent sustained-release properties. The complete release of SR from C_{KP} can be controlled at from 20 to 45 h in anhydrous ethanol. As for the C_{KP} prepared at IPDI dosage of 0.6 g, 22% of SR still remained after 45 h in anhydrous ethanol. Owing to the dual role of Kln as an emulsifier and enhancer and the controllable encapsulation and release performance of microcapsules, this work may have implications for the development of organic–inorganic composite vehicles for drugs and pesticides.

Financial support. The authors wish to acknowledge financial support from the National Natural Science Foundation of China (No. 42062003; No. 41572034), the Guangxi Natural Science Foundation (No. 2019GXNSFBA245052; No. 2018GXNSFAA294012), the Engineering Research Center of Non-metallic Minerals of Zhejiang Province (No. ZD2020K05) and the Zhejiang Biochar Engineering Technology Research Center (No. 2019ZJB08).

References

Amatya S., Park E.J., Park J.H., Kim J.S., Seol E., Lee H. *et al.* (2013) Drug release testing methods of polymeric particulate drug formulations. *Journal of Pharmaceutical Investigation*, **43**, 259–266.

Asghari-Varzaneh E., Shahedi M. & Shekarchizadeh H. (2017) Iron microencapsulation in gum tragacanth using solvent evaporation method. *International Journal of Biological Macromolecules*, **103**, 640–647.

Bago Rodriguez A.M. & Binks B.P. (2019) Capsules from Pickering emulsion templates. *Current Opinion in Colloid & Interface Science*, **44**, 107–129.

Bah M.G., Bilal H.M. & Wang J. (2020) Fabrication and application of complex microcapsules: a review. *Soft Matter*, **16**, 570–590.

Bergaya F. & Lagaly G. (2013) *Handbook of Clay Science*. Newnes, London, UK, 261 pp.

Cai X., Li C., Tang Q., Zhen B., Xie X., Zhu W. *et al.* (2019) Assembling kaolinite nanotube at water/oil interface for enhancing pickering emulsion stability. *Applied Clay Science*, **172**, 115–122.

Cai Y., Wei Q., Huang F., Lin S., Chen F. & Gao W. (2009) Thermal stability, latent heat and flame retardant properties of the thermal energy storage phase change materials based on paraffin/high density polyethylene composites. *Renewable Energy*, **34**, 2117–2123.

Chatterjee S., Tran H.N., Godfred O.-B. & Woo S.H. (2018) Supersorption capacity of anionic dye by newer chitosan hydrogel capsules via green surfactant exchange method. *ACS Sustainable Chemistry & Engineering*, **6**, 3604–3614.

Dai H., Wu J., Zhang H., Chen Y., Ma L., Huang H. *et al.* (2020) Recent advances on cellulose nanocrystals for Pickering emulsions: development and challenge. *Trends in Food Science & Technology*, **102**, 16–29.

Demirbağ S. & Aksoy S.A. (2016) Encapsulation of phase change materials by complex coacervation to improve thermal performances and flame retardant properties of the cotton fabrics. *Fibers and Polymers*, **17**, 408–417.

Dickinson E. (1994) Emulsions and droplet size control. PP. 191–216 in: *Controlled Particle, Droplet and Bubble Formation* (D.J. Wedlock, editor) Butterworth-Heinemann, Oxford, UK.

Fan H. & Striolo A. (2012) Mechanistic study of droplets coalescence in Pickering emulsions. *Soft Matter*, **8**, 9533–9538.

Ganley W.J., Ryan P.T. & van Duijneveldt J.S. (2017) Stabilisation of water-in-water emulsions by montmorillonite platelets. *Journal of Colloid and Interface Science*, **505**, 139–147.

Gonzalez Ortiz D., Pochat-Bohatier C., Cambedouzou J., Bechelany M. & Miele P. (2020) Current trends in Pickering emulsions: particle morphology and applications. *Engineering*, **6**, 468–482.

Hassander H., Johansson B. & Törnell B. (1989) The mechanism of emulsion stabilization by small silica (Ludox) particles. *Colloids and Surfaces*, **40**, 93–105.

Jerri H.A., Jacquemond M., Hansen C., Ouali L. & Erni P. (2016) 'Suction caps': designing anisotropic core/shell microcapsules with controlled membrane mechanics and substrate affinity. *Advanced Functional Materials*, **26**, 6224–6237.

Jiang Z., Yang W., He F., Xie C., Fan J., Wu J. & Zhang K. (2018) Modified phase change microcapsules with calcium carbonate and graphene oxide

https://doi.org/10.1180/clm.2021.15 Published online by Cambridge University Press

shells for enhanced energy storage and leakage prevention. *ACS Sustainable Chemistry & Engineering*, **6**, 5182–5191.
Katepalli H., John V.T. & Bose A. (2013) The response of carbon black stabilized oil-in-water emulsions to the addition of surfactant solutions. *Langmuir*, **29**, 6790–6797.
Korsmeyer R.W., Gurny R., Doelker E., Buri P. & Peppas N.A. (1983) Mechanisms of solute release from porous hydrophilic polymers. *International Journal of Pharmaceutics*, **15**, 25–35.
Kumar G.N., Al-Aifan B., Parameshwaran R. & Ram V.V. (2021) Facile synthesis of microencapsulated 1-dodecanol/melamine-formaldehyde phase change material using *in-situ* polymerization for thermal energy storage. *Colloids and Surfaces A: Physicochemical and Engineering Aspects*, **610**, 125698.
Lavanya M.N., Kathiravan T., Moses J.A. & Anandharamakrishnan C. (2020) Influence of spray-drying conditions on microencapsulation of fish oil and chia oil. *Drying Technology*, **38**, 279–292.
Li C., Fu L., Ouyang J., Tang A. & Yang H. (2015) Kaolinite stabilized paraffin composite phase change materials for thermal energy storage. *Applied Clay Science*, **115**, 212–220.
Li H., Chen H., Li X. & Sanjayan J.G. (2014) Development of thermal energy storage composites and prevention of pcm leakage. *Applied Energy*, **135**, 225–233.
Li W., Zhang X., Wang X., Tang G. & Shi H. (2012) Fabrication and morphological characterization of microencapsulated phase change materials (MicroPCMs) and macrocapsules containing MicroPCMs for thermal energy storage. *Energy*, **38**, 249–254.
Liang S., Li C., Dai L., Tang Q., Cai X., Zhen B. *et al.* (2018) Selective modification of kaolinite with vinyltrimethoxysilane for stabilization of Pickering emulsions. *Applied Clay Science*, **161**, 282–289.
Machado J.P.E., de Freitas R.A. & Wypych F. (2019) Layered clay minerals, synthetic layered double hydroxides and hydroxide salts applied as Pickering emulsifiers. *Applied Clay Science*, **169**, 10–20.
Nguon O., Lagugné-Labarthet F., Brandys F.A., Li J. & Gillies E.R. (2018) Microencapsulation by *in situ* polymerization of amino resins. *Polymer Reviews*, **58**, 326–375.
Ozturk B., Argin S., Ozilgen M. & McClements D.J. (2015) Formation and stabilization of nanoemulsion-based vitamin E delivery systems using natural biopolymers: whey protein isolate and gum arabic. *Food Chemistry*, **188**, 256–263.
Pickering S.U. (1907) Emulsions. *Journal of the Chemical Society, Transactions*, **91**, 2001–2021.
Prasannan A., Tsai H.-C., Chen Y.-S. & Hsiue G.-H. (2014) A thermally triggered *in situ* hydrogel from poly(acrylic acid-*co*-*N*-isopropylacrylamide) for controlled release of anti-glaucoma drugs. *Journal of Materials Chemistry B*, **2**, 1988–1997.
Ravanfar R., Comunian T.A. & Abbaspourrad A. (2018) Thermoresponsive, water-dispersible microcapsules with a lipid–polysaccharide shell to protect heat-sensitive colorants. *Food Hydrocolloids*, **81**, 419–428.
Ritger P.L. & Peppas N.A. (1987) A simple equation for description of solute release I. Fickian and non-Fickian release from non-swellable devices in the form of slabs, spheres, cylinders or discs. *Journal of Controlled Release*, **5**, 23–36.
Rule J.D., Sottos N.R. & White S.R. (2007) Effect of microcapsule size on the performance of self-healing polymers. *Polymer*, **48**, 3520–3529.
Tang Q., Xie X., Li C., Zhen B., Cai X., Zhang G. *et al.* (2019) Medium-chain triglyceride/water pickering emulsion stabilized by phosphatidylcholine–kaolinite for encapsulation and controlled release of curcumin. *Colloids and Surfaces B: Biointerfaces*, **183**, 110414.
Tsoi E.W. (2013) *Formulation Development of a Polymer–Drug Matrix with a Controlled Release Profile for the Treatment of Glaucoma*. PhD thesis, California Polytechnic State University, San Luis Obispo, CA, USA, 77 pp.
Wang X., Zhou W., Cao J., Liu W. & Zhu S. (2012) Preparation of core–shell $CaCO_3$ capsules *via* Pickering emulsion templates. *Journal of Colloid and Interface Science*, **372**, 24–31.
Weng J., Tong H.H.Y. & Chow S.F. (2020) *In vitro* release study of the polymeric drug nanoparticles: development and validation of a novel method. *Pharmaceutics*, **12**, 732.
Xiao Y., Wu B., Fu X., Wang R. & Lei J. (2019) Preparation of biodegradable microcapsules through an organic solvent-free interfacial polymerization method. *Polymers for Advanced Technologies*, **30**, 483–488.
Yang Y., Fang Z., Chen X., Zhang W., Xie Y., Chen Y. *et al.* (2017) An overview of Pickering emulsions: solid-particle materials, classification, morphology, and applications. *Frontiers in Pharmacology*, **8**, 287.
Yi H., Yang Y., Gu X., Huang J. & Wang C. (2015) Multilayer composite microcapsules synthesized by pickering emulsion templates and their application in self-healing coating. *Journal of Materials Chemistry A*, **3**, 13749–13757.
Yin D., Ma L., Liu J. & Zhang Q. (2014) Pickering emulsion: a novel template for microencapsulated phase change materials with polymer–silica hybrid shell. *Energy*, **64**, 575–581.
Yin T., Fu Q., Zhou L. & Fu Y. (2020) Powdered nitrile rubber @ silicon dioxide capsule as the wear modifier of phenolic resin composites under dry friction. *Tribology International*, **151**, 106517.
Yow H.N. & Routh A.F. (2009) Release profiles of encapsulated actives from colloidosomes sintered for various durations. *Langmuir*, **25**, 159–166.
Zhan S., Chen S., Chen L. & Hou W. (2016) Preparation and characterization of polyurea microencapsulated phase change material by interfacial polycondensation method. *Powder Technology*, **292**, 217–222.
Zhang K., Wang Q., Meng H., Wang M., Wu W. & Chen J. (2014) Preparation of polyacrylamide/silica composite capsules by inverse Pickering emulsion polymerization. *Particuology*, **14**, 12–18.
Zhang Z., Tam K.C., Wang X. & Sèbe G. (2018) Inverse Pickering emulsions stabilized by cinnamate modified cellulose nanocrystals as templates to prepare silica colloidosomes. *ACS Sustainable Chemistry & Engineering*, **6**, 2583–2590.
Zhao C.-Y. & Zhang G.H. (2011) Review on microencapsulated phase change materials (MEPCMs): Fabrication, characterization and applications. *Renewable and Sustainable Energy Reviews*, **15**, 3813–3832.
Zhao H., Fei X., Cao L., Zhang B. & Liu X. (2019) Relation between the particle size and release characteristics of aromatic melamine microcapsules in functional textile applications. *RSC Advances*, **9**, 25225–25231.
Zhao J., Long J., Du Y., Zhou J., Wang Y., Miao Z. *et al.* (2020) Recyclable low-temperature phase change microcapsules for cold storage. *Journal of Colloid and Interface Science*, **564**, 286–295.

https://doi.org/10.1180/clm.2021.15 Published online by Cambridge University Press